



# Effects of brazing temperature on microstructure and mechanical performance of $\text{Al}_2\text{O}_3/\text{AgCuTi}/\text{Fe-Ni-Co}$ brazed joints



Yongtong Cao, Jiazhen Yan\*, Ning Li, Yi Zheng, Chenglai Xin

School of Manufacturing Science and Engineering, Sichuan University, Chengdu, 610065, China

## ARTICLE INFO

### Article history:

Received 6 February 2015

Received in revised form

24 July 2015

Accepted 25 July 2015

Available online 29 July 2015

### Keywords:

$\text{Al}_2\text{O}_3$  ceramic/ Fe–Ni–Co joint

Joint strength

Microstructure

Reaction layer

## ABSTRACT

$\text{Al}_2\text{O}_3/\text{Fe-Ni-Co}$  joints are achieved using Ag–Cu–8Ti filler alloy, and the dependence of the joint microstructure and mechanical performance on the brazing temperature has been studied by means of SEM, EDS, XRD and tensile test. The results show that the brazing seam is composed of TiO,  $\text{Ti}_3\text{Al}$ , Ag (s, s), Cu (s, s), (Cu, Ni) and  $\text{Ni}_4\text{Ti}_3$  phases. A layer of  $\text{Ti}_3\text{Al}$  and TiO products is observed at the  $\text{Al}_2\text{O}_3/\text{AgCuTi}$  interface and the fracture testing indicates that the thickness of the reaction layer plays a critical role in the joint strength. The joint strength firstly increases and then declines with the thickness of the ( $\text{Ti}_3\text{Al} + \text{TiO}$ ) layer increasing, and the formation of the cracks is ascribed to the existence of  $\text{Ti}_3\text{Al}$  phase. The thermokinetic analysis for the interfacial reaction between  $\text{Al}_2\text{O}_3$  and AgCuTi show that the Gibbs free energy equals  $-88.939$  kJ/mol for forming  $\text{Ti}_3\text{Al}$  and TiO phases, and the growth rate of the reaction layer mainly depends on the diffusion rate of Ti across the formed reaction layer. Meanwhile, the quantitative relationship among brazing temperature, holding time and reaction layer thickness has been established.

© 2015 Elsevier B.V. All rights reserved.

## 1. Introduction

Ceramic materials are widely used in many areas of industries due to a combination of high-temperature resistance, corrosion resistance and abrasion resistance. However, the application of ceramic is always limited by its poor toughness and machinability, so in order to make its excellent properties fully utilized in practical applications, ceramic materials are usually joined with metals, which is Fe–Ni–Co alloy in this paper, to manufacture a component. The common methods to join ceramics and metals can be classified into two kinds: one is the method of surface metallization with subsequent Ni plating of ceramic surface before brazing, and the other is active brazing by using active filler containing a small amount of Ti, Zr or Hf elements. The method of surface metallization of ceramic has been a standard industrial process, but the inadequacies of complex process and time-consuming limit its far-ranging applications in engineering. To simplify operation process and shorten the production cycle, a method of directly brazing metal to ceramic with the active filler alloy has been appreciated.

The series of AgCuTi filler alloy are applied to the connections of various ceramics or ceramics to metals, and the effect of reaction process and reaction products between the ceramic and active filler on the joint strength have attracted the most attention in recent years [1–3]. Nanoindentation method is introduced for probing the mechanical properties of reaction phases of  $\text{Si}_3\text{N}_4/\text{AgCuTi}/\text{SiC-Si}_3\text{N}_4$  joint and the digital image correlation (DIC) technique is applied to clarified the strengthening mechanism of the joint [4]. The ZrB<sub>2</sub>–SiC composites (ZS) are also joined using an Ag–Cu/Ti filler alloy [5], and the result shows that the mechanical properties of ZS/ZS joint are improved by interfacial TiB accommodation due to the reduction of the coefficient of CTE mismatch. For  $\text{Al}_2\text{O}_3/\text{Ag-Pd-Ti/Kovar}$  joint [6], the effect of Ti content on the interfacial microstructure and mechanical properties shows that the type of titanium oxide are affected by the thickness of Ti layer, and the joint strength are influenced by the thickness of reaction layer and residual Ti layer. M. Brochu [7] studied the active brazing of  $\text{Si}_3\text{N}_4$  ceramic and FA-129 alloy, and they found a reaction layer formed at  $\text{Si}_3\text{N}_4/\text{Cu}$  interface and discussed the relation between the thickness and brazing time. The  $\text{Al}_2\text{O}_3/\text{Al}_2\text{O}_3$  joint can be achieved using Ag–Cu–Ti + B +  $\text{TiH}_2$  composite filler [8], the results show that the addition of B powders in composite filler increases TiB whiskers content, but decreases the thickness of  $\text{Ti}_3(\text{Cu,Al})_3\text{O}$  layer, while the higher  $\text{TiH}_2$  powders content thickens  $\text{Ti}_3(\text{Cu,Al})_3\text{O}$  layer.

\* Corresponding author.

E-mail address: [yanjiazhen@scu.edu.cn](mailto:yanjiazhen@scu.edu.cn) (J. Yan).

It is well accepted that during the active brazing process, the active element, such as Ti, in the molten brazing filler is absorbed to the surface of ceramic and forming a layer of reaction product with ceramic at the interface. The morphology and the properties of the reaction layer, which are determined by brazing process, play important roles in the joint strength. However, the relationship of brazing temperature, holding time and thickness of the reaction layer and the discussion of growth process of the reaction layer are rarely mentioned. In order to identify the dependence of seam microstructure and the joint strength on the brazing temperature, holding time and thickness of the reaction layer, AgCuTi filler alloy is applied to braze  $\text{Al}_2\text{O}_3$  and Fe–Ni–Co at different temperatures for various times in the present paper. The study also aims to investigate the reaction between AgCuTi filler with  $\text{Al}_2\text{O}_3$  ceramic, the controlling factors in the growth of the reaction layer, the reasons for the change of joint strength and the mechanisms of the formation of the microcracks during tensile testing.

## 2. Experimental

The ceramic and metal used in this work were 95 wt%  $\text{Al}_2\text{O}_3$  ceramic and Fe–33 wt% Ni–15 wt% Co alloy plates. Fe–Ni–Co alloy plates were chosen as another matrix treated with the surface nickel-plated to ensure a favorable spreadability of the brazing filler on it.  $\text{Al}_2\text{O}_3$  ceramic and Fe–Ni–Co alloy was assembled (shown as Fig. 1) after their surface for brazing were coated by a commercial paste Ag–25.92 wt% Cu–7.89 wt% Ti filler alloy (Lucas-Milhaupt, Inc).

Due to the high Ti content (7.89 wt%) in the used AgCuTi filler alloy, the samples were performed in a horizontal vacuum at a pressure of  $3.0 \times 10^{-3}$  Pa to avoid the oxidation of active Ti during heating. The heating curve was shown in Fig. 2. A heating rate of  $10^\circ\text{C}/\text{min}$  was set, which could effectively reduce the temperature gradient of samples to prevent the generation of internal stress. Heat preservation was set at  $450^\circ\text{C}$  holding for 30 min to make organic adhesive in AgCuTi filler fully decompose before being pumped. All samples were preheated to  $750^\circ\text{C}$  and held for 30 min before they were heated to the brazing temperature to reduce the time delay between the true specimen temperature and program temperature. In order to reduce the temperature gradient of samples and prevent the generation of stress, the sample was cooled at a rate of  $3^\circ\text{C}/\text{min}$  from the brazing temperature to  $720^\circ\text{C}$  and subsequently cooled inside the furnace to room temperature. The tensile strength of brazed joint was determined by RGX-M300 electronic universal testing machine with a speed of 0.5 mm/min.

For the characterization of metallographic structure, the samples were ground to 10 mm in thickness along the direction

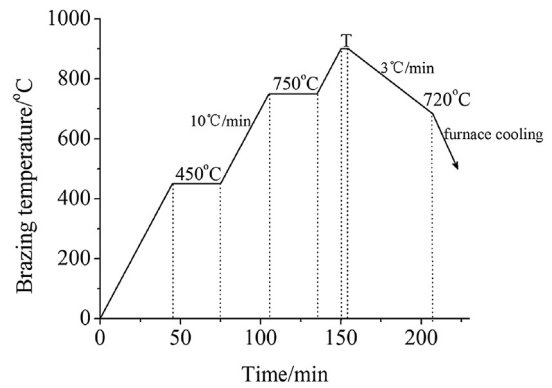


Fig. 2. The programming heating curve during brazing process.

perpendicular to the seam by diamond discs before being etched. Microstructure and reaction phases were examined by means of the HITACHI S-4800 scanning electron microscope (SEM) equipped with an energy dispersive X-ray spectrometer (EDS). The different phases were identified using the X'Pert PRO X-ray diffractometer (XRD).

## 3. Results and discussion

### 3.1. Microstructures and interfaces

The microstructures of the brazing seam detected by SEM are shown in Fig. 3. The results indicate that the joints are mainly composed of three parts: an interfacial reaction layer with a thickness of approximately  $0.8\text{--}1.8\ \mu\text{m}$  adjacent to  $\text{Al}_2\text{O}_3$  ceramic, a brazing seam zone consisting of banded structures, lump phases and concave phases, and an interfacial reaction zone adjacent to Fe–Ni–Co alloy. Fig. 3(a) shows an interfacial reaction layer of about  $0.8\ \mu\text{m}$  in thickness between  $\text{Al}_2\text{O}_3$  ceramic and AgCuTi filler alloy, which indicates the occurrence of metallurgical reactions between  $\text{Al}_2\text{O}_3$  and AgCuTi filler. However, the faying interface between AgCuTi and Fe–Ni–Co is clear, because the dissolution of Fe–Ni–Co towards AgCuTi is largely limited at such a low temperature of  $870^\circ\text{C}$ . In comparison, an interfacial reaction zone with a tortuous joining line adjacent to Fe–Ni–Co alloy is observed in Fig. 3(b), which is benefited from the rise of brazing temperature ( $890^\circ\text{C}$ ). In addition, the reaction layer at  $\text{Al}_2\text{O}_3/\text{AgCuTi}$  interface in Fig. 3(b) is continuous and the thickness increases to  $1.4\ \mu\text{m}$  due to the violent interfacial metallurgical reaction that also caused by the rise of brazing temperature. Comparing the three samples brazed at different temperatures, the thickness of reaction layer adjacent to  $\text{Al}_2\text{O}_3$  ceramic increases with the rise of brazing temperature, and it reaches  $1.7\ \mu\text{m}$  at a brazing temperature of  $910^\circ\text{C}$ , as shown in black-bordered box in Fig. 3(c).

Fig. 4 shows the elemental diffusion of the cross section of  $\text{Al}_2\text{O}_3/\text{AgCuTi}/\text{Fe–Ni–Co}$  joint. The results reveal that Ti element aggregates to  $\text{Al}_2\text{O}_3$  surface (zone A) and in the banded structure (zone C), and Ni distributes in the whole brazing joint and present higher concentration in banded structure and near Fe–Ni–Co alloy. It is noted that Al and O aggregate in the layer at  $\text{Al}_2\text{O}_3/\text{AgCuTi}$  interface and Cu distributes in the whole brazing seam.

In order to identify the formed phases in the  $\text{Al}_2\text{O}_3/\text{AgCuTi}/\text{Fe–Ni–Co}$  brazing seam, an EDS analysis was conducted to investigate the composition of the phases as shown in Fig. 5. Table 1 shows the EDS analysis results of the  $\text{Al}_2\text{O}_3/\text{AgCuTi}/\text{Fe–Ni–Co}$  joint in Fig. 5. It can be seen that the lump phases (as marked by “D”) are Cu-rich and the concave phases are Ag-rich. As a result of

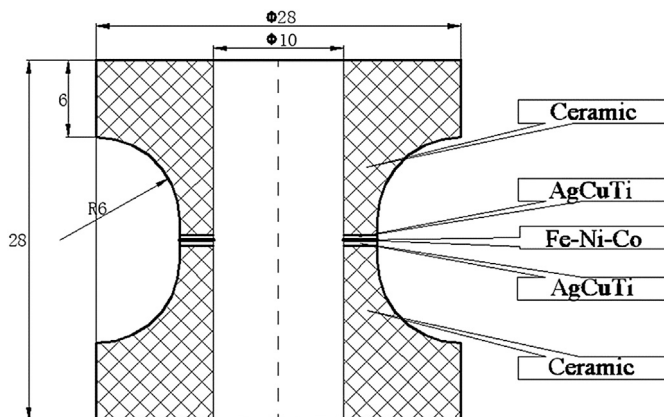


Fig. 1. Sketch of assembling jig for samples.

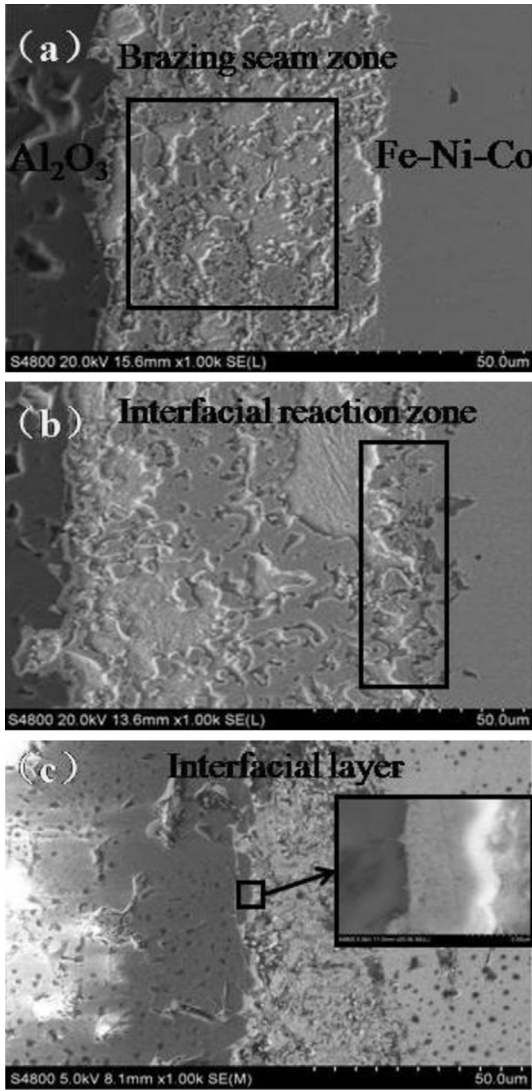


Fig. 3. SEM micrographs of  $\text{Al}_2\text{O}_3/\text{AgCuTi}/\text{Fe-Ni-Co}$  joints at different brazing temperature (a) 870 °C; (b) 890 °C; (c) 910 °C.

the contents of Ti, Ni elements far more than Cu, it can be inferred that Ti probably prefers to interact with Ni to form  $\text{Ni}_4\text{Ti}_3$  phase rather than Cu (as marked by “C”). (Cu, Ni) solid solutions (as marked by “E”) forms adjacent to Fe–Ni–Co alloy, because lots of Ni

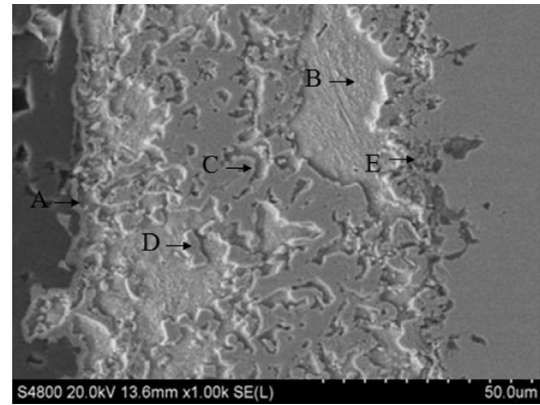


Fig. 5. SEM micrograph of  $\text{Al}_2\text{O}_3/\text{AgCuTi}/\text{Fe-Ni-Co}$  joint (brazed at 890 °C).

from the molten Fe–Ni–Co meet partial Cu-rich liquid from the melting of AgCuTi [9]. Therefore, the banded structures are  $\text{Ni}_4\text{Ti}_3$  phases and the interfacial reaction zone adjacent to Fe–Ni–Co alloy are mainly consisting of (Cu, Ni) solid solutions. Active element Ti is adsorbed onto  $\text{Al}_2\text{O}_3$  surface preferentially after AgCuTi melt into liquid due to its high chemical activity [10], eventually leading to the formation of  $\text{Ti}_3\text{Al}$  and TiO at the  $\text{Al}_2\text{O}_3/\text{AgCuTi}$  interface (as marked by “A”) through the following metallurgical reaction:



The standard enthalpy of formation, absolutely entropy and heat capacity of Ti,  $\text{Al}_2\text{O}_3$  and TiO can be detected from the thermodynamic manuals [11]. However, for those thermodynamic data which cannot be indexed directly from the manuals, such as the free energy of  $\text{A}_x\text{B}_y$  alloy, we can regard it as a binary system consisting of X moles of A and Y moles of B [12], and its free energy can be approximately estimated as:

$$\Delta G = X\bar{G}_A + Y\bar{G}_B \quad (2)$$

$$\bar{G}_i = G_i^0 + RT\ln a_i \quad (i = A, B) \quad (3)$$

$$a_i = \gamma_i x_i \quad (4)$$

Where  $G_i^0$  (kJ/mol) and  $a_i$  are the partial free enthalpy and activity of i substance,  $x_i$  and  $\gamma_i$  are the mole fraction and activity coefficient of i component. What need alludes is,  $\gamma_i$  can be calculated by the formula proposed by Srikanth [13]. By calculating, relevant

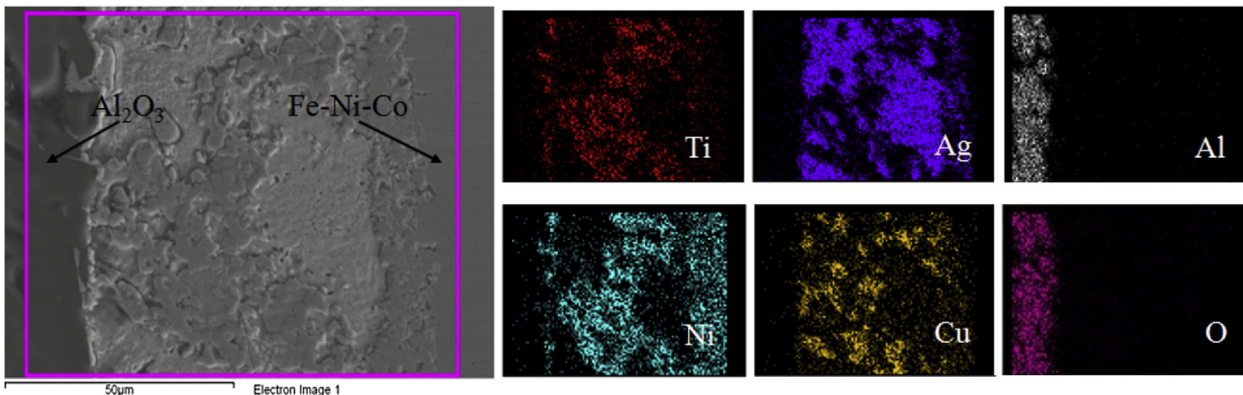


Fig. 4. Component analysis of the cross section of  $\text{Al}_2\text{O}_3/\text{AgCuTi}/\text{Fe-Ni-Co}$  joint (brazed at 890 °C).



**Table 1**

The EDS analysis results of different areas in Fig. 5.

Zones	Element (at. %)							
	O	Al	Ti	Fe	Co	Ni	Cu	Ag
A	25.83	23.45	8.18	0.34	0.18	22.23	17.84	1.96
B	0.74	0.12	0.18	–	0.59	2.72	8.81	87.02
C	1.00	0.49	16.76	0.52	0.22	49.36	10.57	21.09
D	0.75	0.64	1.73	–	–	9.84	85.64	1.39
E	0.69	0.23	1.41	4.60	1.80	24.87	66.06	0.35

**Table 2**

Thermodynamic data of relevant reactants and reaction products.

Chemical compounds	$\Delta G_{890^\circ\text{C}}$ (kJ/mol)
Ti <sub>3</sub> Al	–296.928
TiO	–599.700
Al <sub>2</sub> O <sub>3</sub>	–1805.743
Ti	–55.386

parameters of Ti and Al components can be obtained at 890 °C as follows:  $\gamma_{\text{Ti}} = 0.721$ ,  $\gamma_{\text{Al}} = 0.0107$ ,  $x_{\text{Ti}} = 0.75$ ,  $x_{\text{Al}} = 0.25$ ,  $a_{\text{Ti}} = 0.5408$  and  $a_{\text{Al}} = 0.0027$ . The free energies of Ti<sub>3</sub>Al, TiO, Ti and Al<sub>2</sub>O<sub>3</sub> are shown in Table 2. Since the change of the system free energy is  $-88.739$  kJ/mol ( $\Delta G < 0$ ), the formation of titanium oxide (TiO) and titanium-aluminum intermetallic compound (Ti<sub>3</sub>Al) at Al<sub>2</sub>O<sub>3</sub>/AgCuTi interface is thermodynamically feasible.

The interfacial structure of the samples can be expressed as Al<sub>2</sub>O<sub>3</sub>/TiO + Ti<sub>3</sub>Al/Ag (s, s) + (Cu, Ni)/Ag (s, s) + Cu (s, s) + Ni<sub>4</sub>Ti<sub>3</sub>/Fe–Ni–Co. According to the phase diagram of AgCuTi ternary alloy, the filler tends to separate into two immiscible liquid phases upon melting, one liquid phase is rich in Ag and the other is rich in both Cu and Ti [14]. When the reaction starts, Ni<sub>4</sub>Ti<sub>3</sub> phase generates immediately because of the reaction between active element Ti and free Ni, leading to Cu-rich phase forming in the brazed seam zone instead of (Cu, Ni) phase. Meanwhile, active element Ti in the molten filler is adsorbed to Al<sub>2</sub>O<sub>3</sub> surface due to its high chemical activity, thus (Ti<sub>3</sub>Al + TiO) layer is formed at the Al<sub>2</sub>O<sub>3</sub>/AgCuTi interface through the fore-mentioned metallurgical reaction (Eq. (1)). The high contents of Ni beside Fe–Ni–Co alloy can react with Cu liquid to generate (Cu, Ni) solid solution containing a small amount of Fe and Co. Lastly, banded structure was surrounded by liquid Ag and surplus liquid Cu until the end of the reaction.

### 3.2. Mechanical performance

Al<sub>2</sub>O<sub>3</sub> ceramic/Fe–Ni–Co alloy are brazed using AgCuTi filler alloy at different temperatures, and the average tensile strength of six samples for each temperature are obtained as shown in Fig. 6.

According to Fig. 6, it can be seen that the joint strength with a little discrete nature firstly increases and then declines with brazing temperature increase, and the highest tensile strength of 78 MPa is obtained when the sample is brazed at 890 °C for 5 min. In order to find the reasons for the change in joint strength, the relations of brazing temperature, holding time, joint strength and thickness of reaction layer are discussed. The thickness relationship of reaction layer at the Al<sub>2</sub>O<sub>3</sub>/AgCuTi interface under different temperature conditions was shown in Fig. 7. Comparing the tensile results in Fig. 6 and the reaction layer results in Fig. 7, it is feasible to conclude that the strength of Al<sub>2</sub>O<sub>3</sub>/AgCuTi/Fe–Ni–Co joint firstly increases and then declines with the reaction layer thickness increases.

It is generally believed that the interfacial reaction of ceramic-metal is controlled by the diffusion in between ceramic and metal, and the growth curve of the reaction layer keeps a parabolic

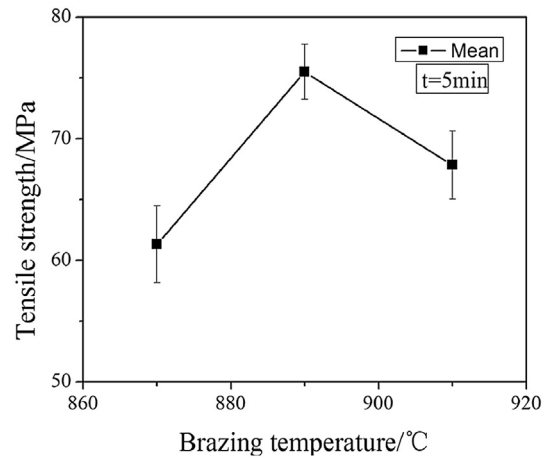


**Fig. 6.** Influence of the brazing temperature on the tensile strength of Al<sub>2</sub>O<sub>3</sub>/AgCuTi/Fe–Ni–Co joint.

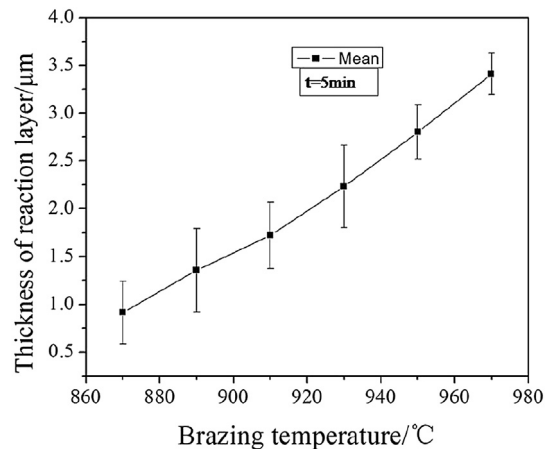


**Fig. 7.** Influence of the brazing temperature on the thickness of reaction layer (the brazing time is 5 min).

tendency. Thus the thickness of the reaction layer can be expressed as [15]:

$$X = Kt^{0.5} \quad (5)$$

$$K = k_0 \exp(-Q/RT) \quad (6)$$

Where  $X$  (m) is the thickness of reaction layer,  $K$  (m<sup>2</sup>/s) is the reaction rate constant,  $Q$  (kJ/mol) and  $k_0$  (m<sup>2</sup>/s) are the activation energy and the pre-exponential factor, and  $R$  is gas constant equaled to 8.314 J/(K mol). The  $K_0$  and  $Q$  can be estimated as  $2.2616 \times 10^{-1}$  m<sup>2</sup>/s and 143.85 kJ/mol, respectively, from the results of the linear fitting shown in Fig. 8(a). The relationship among thickness of the reaction layer, holding time and brazing temperature can be written as:

$$X = 2.2616 \times 10^{-1} \exp\left(-143.85 \times 10^3 / 8.314T\right) \times t^{0.5} \quad (7)$$

Where  $X$  (m) is the thickness of reaction layer,  $T$  (K) is the brazing temperature and  $t$  (s) is the brazing time. To further prove the correctness of Eq. (7), Al<sub>2</sub>O<sub>3</sub> ceramic and Fe–Ni–Co alloy are brazed using AgCuTi filler for 1 min, 10 min, 20 min and 30 min at 890 °C. Fig. 8(b) displays the theoretical values is very close to the

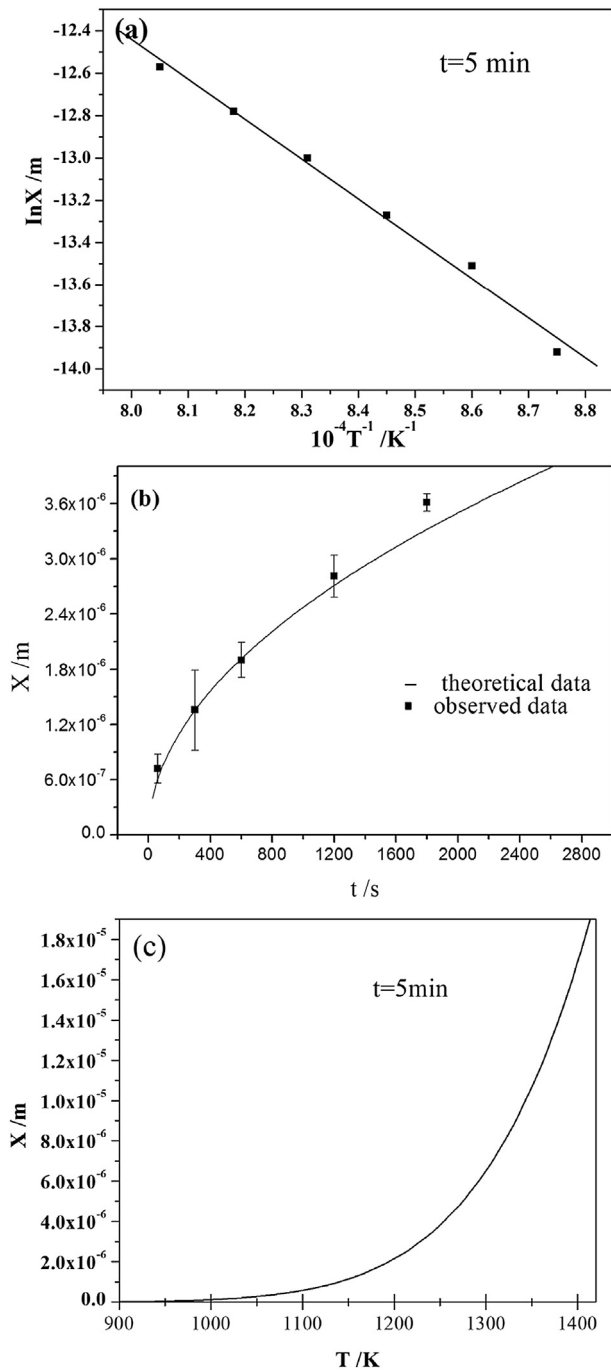


**Fig. 8.** (a) Linear fitting results of data from Fig. 7; (b) The comparison of theoretical and experimental data; (c) Curvilinear relationship of brazing temperature and thickness of reaction layer.

measured mean counterparts. So it can be confirmed that Eq. (7) can be used to evaluate the actual situation, and thus the relationship of brazing temperature and the thickness of reaction layer was presented in Fig. 8(c).

The interaction between  $Al_2O_3$  ceramic and AgCuTi filler alloy is a reaction-diffusion process [15], consisting of the diffusion of Ti atoms across the reaction layer and the metallurgical reaction between Ti and  $Al_2O_3$ . So the extracted activation energy ( $Q$ ) can be considered as the reaction-diffusion activation energy that includes the activation energy of the Ti diffusion and the activation energy to transition state of the reaction. The reaction between Ti in the

molten AgCuTi filler and  $Al_2O_3$  stem from the adsorption of Ti onto the surface of  $Al_2O_3$  in two steps [16]: the physical adsorption firstly stems from the Van der Waals forces between Ti and surface atom of  $Al_2O_3$  ceramic, and then the chemical adsorption occurs when the activation energy is so high to counteract the atomic binding energy. The initial reaction layer at the  $Al_2O_3/AgCuTi$  interface can be obtained as reaching the activation energy to transition state. However, the formed reaction layer becomes a barrier-layer of further reaction between Ti and  $Al_2O_3$ . So the Ti atoms have to pass through the formed reaction layer by diffusion to keep the further reaction. The diffusion of Ti atoms in the formed layer achieves by vacancy diffusion or diffusing along the grain boundary [17].

The growth rate of reaction layer lies on the diffusion rate of Ti atoms across the reaction layer and the rate of the chemical reaction. It can be observed that the growth rate of reaction layer declines with the increase of brazing time as shown in Fig. 8 (b). This phenomenon indicates that the diffusion rate of Ti atoms across the reaction layer is less than the rate of the chemical reaction during brazing, that is, the growth rate of reaction layer mainly depends on the diffusion rate of Ti atoms across the formed reaction layer.

The reasons for the change in joint strength can be described as below. The reaction layer at the  $Al_2O_3/AgCuTi$  interface can effectively realize the combination of ceramic and brazing seam in a form of chemical bonds [18,19]. Practically, the higher brazing temperature is, the more Ti concentrates near  $Al_2O_3$  ceramic and the faster Ti atom diffuses across the reaction layer. So Ti cannot diffuse largely to the surface of  $Al_2O_3$  ceramic at  $870$  °C. When the temperature rises to  $890$  °C, the increase in thickness of reaction layer leads to the improvement of joint strength. Although the reaction layer benefits the strength of the joint, the joint strength decreased due to the poor strength of its own when the temperature rises continually. Therefore, the thickness of the reaction layer should be controlled in a reasonable range to ensure the higher joint strength, which can be achieved by tuning the parameters of Eq. (7) in the practical production.

### 3.3. Fracture analysis

Fig. 9(a) shows the fracture morphology of  $Al_2O_3/AgCuTi/Fe-Ni-Co$  joint. It can be seen that the  $Al_2O_3$  fracture surface is stereoscopic and angular, exhibiting the typical characteristic of intergranular fracture. Fig. 9(b) shows that cracks form at the interface between  $Al_2O_3$  and AgCuTi and there are no cracks formed at the reaction zone of Fe-Ni-Co/AgCuTi and in the brazing seam. This phenomenon indicates that the initiation of the cracks in the joints relate to the reaction product formed at  $Al_2O_3/AgCuTi$  interface under this experimental condition. When the external load exceeds the intensity of local stress around  $Ti_3Al$  particle, which is hard and brittle [20], microcracks generate because of the existing of stress between  $Ti_3Al$  phase and TiO phase due to the differences in elastic-plastic. Microcracks aggregate and grow up with the loading, and then propagate into the  $Al_2O_3$  grain boundaries as shown in Fig. 9(b). Although  $Ni_4Ti_3$  compounds could be also formed in the brazing seam, these compounds are not so brittle and have a certain plasticity [21]. Therefore, no crack is observed in the brazing seam. In addition, the product phases in the brazing seam are reconfirmed by XRD analysis of the fracture surface of  $Al_2O_3/AgCuTi/Fe-Ni-Co$  joint as shown in Fig. 10, and the insets in Fig. 10 are the magnification of the peaks of  $Ti_3Al$ , TiO and  $Ni_4Ti_3$ . Besides the well-defined peaks of  $Al_2O_3$ , Ti-Al inter-metallic compounds ( $Ti_3Al$ ), titanium oxide (TiO), Ni-Ti inter-metallic compounds ( $Ni_4Ti_3$ ) and phases of enrichment (Ag(s, s) and Cu(s, s)) are found. Combining the XRD results with the composition of the phases in the seam detected by EDS, it is verified that the brazing seam zone is composed of  $Ni_4Ti_3(R-3)$ , Ag(s, s) and Cu(s, s)

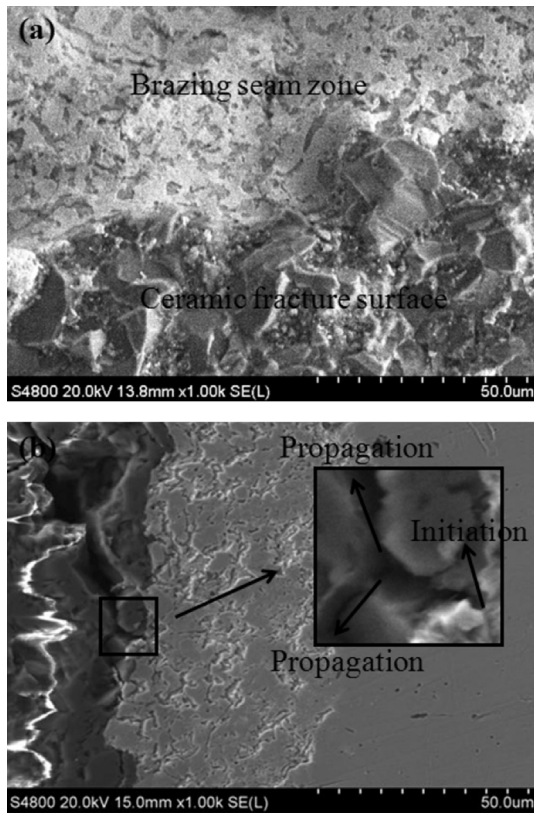


Fig. 9. Tensile fracture morphology of  $\text{Al}_2\text{O}_3/\text{AgCuTi}/\text{Fe-Ni-Co}$  joint.

and the interfacial layer is mainly composed of  $\text{TiO}$  (A2/m) and  $\text{Ti}_3\text{Al}$  (P63/mmc).

#### 4. Conclusion

$\text{Al}_2\text{O}_3$  ceramic are brazed to  $\text{Fe-Ni-Co}$  alloy using  $\text{AgCuTi}$  filler alloy at different temperatures. The primary conclusions are summarized as below:

1. With the brazing temperature increasing, the strength of  $\text{Al}_2\text{O}_3/\text{AgCuTi}/\text{Fe-Ni-Co}$  joint firstly increases and then declines, and the joints with a  $1.4 \mu\text{m}$  thick reaction layer at the  $\text{Al}_2\text{O}_3/\text{AgCuTi}$  interface, which are obtained by brazing at  $890^\circ\text{C}$  for 5 min, have the highest tensile strength of 78 MPa.
2. The strength of  $\text{Al}_2\text{O}_3/\text{AgCuTi}/\text{Fe-Ni-Co}$  joints firstly increase and then decline with thickness of the reaction layer increasing. The relationship of the thickness of reaction layer, holding time and brazing temperature can be expressed as  $X = 2.2616 \times 10^{-1} \exp(-143.85 \times 10^3 / 8.314 T) \times t^{0.5}$ , where  $X$  (m) is the thickness of reaction layer,  $T$  (K) is the brazing temperature and  $t$  (s) is the brazing time. The quantitative relationship means the joint strength can be controlled by the thickness of reaction layer at the  $\text{Al}_2\text{O}_3/\text{AgCuTi}$  interface in practical production.
3. The growth of reaction layer between  $\text{Al}_2\text{O}_3$  and  $\text{AgCuTi}$  is a reaction-diffusion process, and the growth rate of reaction layer mainly depends on the diffusion rate of Ti atom across the formed reaction layer.
4. The microstructure of  $\text{Al}_2\text{O}_3/\text{AgCuTi}/\text{Fe-Ni-Co}$  joint can be expressed as  $\text{Al}_2\text{O}_3/\text{Ti}_3\text{Al} + \text{TiO}/\text{Ag} (s, s) + (\text{Cu}, \text{Ni})/\text{Ag} (s, s) + \text{Cu} (s, s) + \text{Ni}_4\text{Ti}_3/\text{Fe-Ni-Co}$  and the reaction for forming  $\text{Ti}_3\text{Al}$  phase and  $\text{TiO}$  phase is validated by thermodynamics analysis.

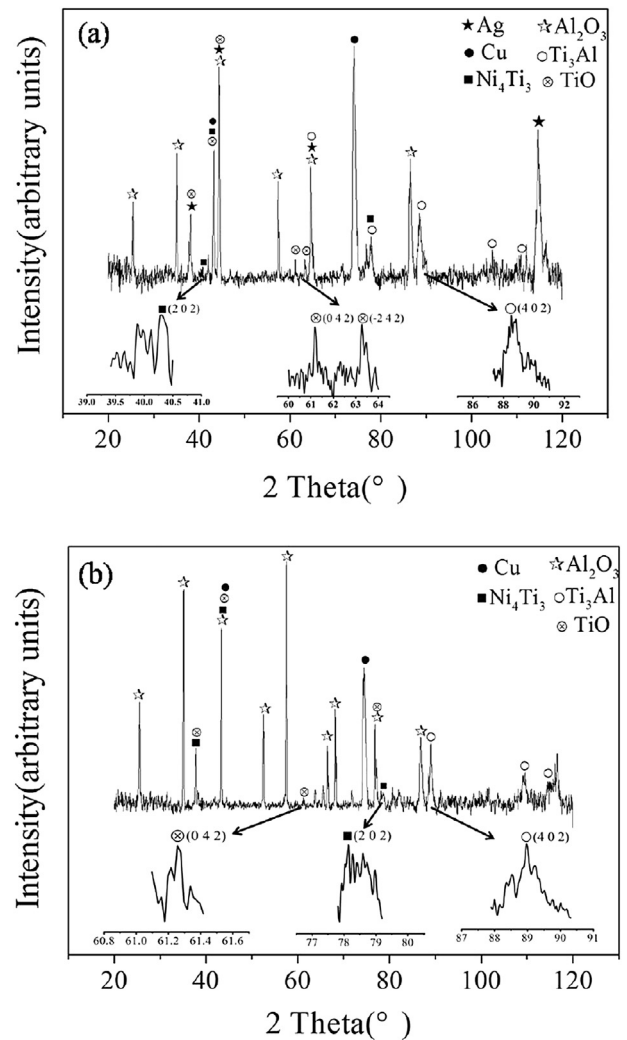


Fig. 10. XRD patterns from the fracture surface of  $\text{Al}_2\text{O}_3/\text{AgCuTi}/\text{Fe-Ni-Co}$  joint (a) XRD pattern of  $\text{Fe-Ni-Co}$  side, (b) XRD pattern of  $\text{Al}_2\text{O}_3$  side.

The microcracks firstly form at the interface between  $\text{Ti}_3\text{Al}$  phase and  $\text{TiO}$  phase, and then propagate into the  $\text{Al}_2\text{O}_3$  ceramic along grain boundaries after their aggregation and growth.

#### Acknowledgments

The authors thank Mr. Shang Jianli, Mr. Yang Rui and Mr. Zhang Fu for their help in the experiments.

#### References

- [1] R. Asthana, M. Singh, J. Martinez-Fernandez, Joining and interface characterization of in situ reinforced silicon nitride, *J. Alloys Compd.* 552 (2013) 137–145.
- [2] P. Prakash, T. MoHandas, P. Dharmar, Microstructural characterization of  $\text{SiC}$  ceramic and  $\text{SiC}$ -metal active metal brazed joints, *Scr. Mater.* 52 (11) (2005) 1169–1173.
- [3] M.X. Yang, T.S. Lin, P. He,  $\text{Cu}+\text{TiB}_2$  composite filler for brazing  $\text{Al}_2\text{O}_3$  and  $\text{Ti-6Al-4V}$  alloy, *J. Alloys Compd.* 512 (2012) 282–289.
- [4] Y.M. He, Y. Sun, J. Zhang, An analysis of deformation mechanism in the  $\text{Si}_3\text{N}_4\text{-AgCuTi} + \text{SiCp-Si}_3\text{N}_4$  joints by digital image correlation, *J. Eur. Ceram. Soc.* 23 (2013) 157–164.
- [5] W.Q. Yang, T.S. Lin, Microstructural investigation of in situ  $\text{TiB}$  whiskers array reinforced  $\text{ZrB}_2\text{-SiC}$  joint, *J. Alloys Compd.* 527 (2012) 117–121.
- [6] W.W. Zhu, J.C. Chen, C.H. Jiang, Effects of Ti thickness on microstructure and mechanical properties of alumina-Kovar joints brazed with  $\text{Ag-Pd/Ti}$  filler, *Ceram. Int.* 40 (2014) 5699–5705.

- [7] M. Brochu, M.D. Pugh, R.A.L. Drew, Brazing silicon nitride to an iron-based intermetallic using a copper interlayer, *Ceram. Int.* 30 (2004) 901–910.
- [8] M.Y. Yang, T.S. Ling, P. He, Microstructure evolution of  $Al_2O_3/Al_2O_3$  joint brazed with Ag-Cu-Ti + B +  $TiH_2$  composite filler, *Ceram. Int.* 38 (2012) 289–294.
- [9] R.K. Shiue, S.K. Wu, C.H. Chan, The interfacial reactions of infrared brazing Cu and Ti with two silver-based braze alloys, *J. Alloys Compd.* 372 (2004) 148–157.
- [10] J.L. Shang, J.Z. Yan, N. Li, Brazing W and Fe-Ni-Co alloy using Ag-28Cu and Ag-27Cu-3.5Ti fillers, *J. Alloys Compd.* 611 (2014) 91–95.
- [11] Y. Liang, Y. Che, *Handbook of Thermodynamics of Inorganic Substance*, Dong Bei University Press, 1994.
- [12] Z.Y. Xu, *Thermodynamics of Metal Materials*, Science Press, 1981.
- [13] D.J. Chronister, S.W. Scott, D.R. Stickle, Induction skull melting of titanium and other reactive alloy, *J. Metals* 38 (9) (1986) 51–54.
- [14] M. Paulasto, F.J.J. van Loo, J.K. Kivilahti, Thermodynamic and experimental study of Ti-Ag-Cu alloys, *J. Alloys Compd.* 220 (1995) 136–141.
- [15] D. Janickovic, P. Sebo, P. Duhaj, The rapidly quenched Ag-Cu-Ti ribbons for active joining of ceramics, Original Research Article, *Mater. Sci. Eng. A* 304 (2001) 569–573.
- [16] S. Roy Morrison, *The Chemical Physics of Surface*, Plenum Press, 1997.
- [17] P.G. Shewmon, *Diffusion in Solids*, McGraw-Hill, New York, 1997.
- [18] C. Wu, Z. Wang, Q.G. Li, Mechanical properties and microstructure evolution of Ti/ $Al_2O_3$ cermet composite with CeO<sub>2</sub>addition, *J. Alloys Compd.* 617 (2014) 729–733.
- [19] W.M. Tang, Z.X. Zheng, A study of the solid state reaction between silicon carbide and iron, *Mater. Chem. Phys.* 74 (3) (2002) 236–241.
- [20] W. Li, X.G. Wang, Overview of studies on the embrittlement of titanium and aluminide, *Physics* 27 (11) (1998) 676–679.
- [21] O. Paiva, M. Barbosa, Production, Bonding strength and electrochemical behaviour of commercially pure Ti/ $Al_2O_3$ brazed joints, *J. Mater. Sci.* 32 (3) (1997) 653–659.